The Pollution-Routing Problem

Tolga Bektaş [a,*], Gilbert Laporte [b]

[a] School of Management and Centre for Operational Research, Management Science and Information Systems (CORMSIS), University of Southampton, Southampton, Highfield SO17 1BJ, United Kingdom
[b] Canada Research Chair in Distribution Management and Interuniversity Research Centre on Enterprise Networks, Logistics, and Transportation (CIRRELT), HEC Montréal, 3000 chemin de la Côte-Sainte-Catherine, Montréal, Canada H3T 2A7

ARTICLE INFO

ABSTRACT

The amount of pollution emitted by a vehicle depends on its load and speed, among other factors. This paper presents the Pollution-Routing Problem (PRP), an extension of the classical Vehicle Routing Problem (VRP) with a broader and more comprehensive objective function that accounts not just for the travel distance, but also for the amount of greenhouse emissions, fuel, travel times and their costs. Mathematical models are described for the PRP with or without time windows and computational experiments are performed on realistic instances. The paper sheds light on the tradeoffs between various parameters such as vehicle load, speed and total cost, and offers insight on economies of 'environmental-friendly' vehicle routing. The results suggest that, contrary to the VRP, the PRP is significantly more difficult to solve to optimality but has the potential of yielding savings in total cost.

1. Introduction

Transportation has hazardous impacts on the environment, such as resource consumption, land use, acidification, toxic effects on ecosystems and humans, noise, and the effect induced by Greenhouse Gas (GHG) emissions (Knörr, 2008). Among these, GHG and in particular CO_2 emissions are the most concerning as they have direct consequences on human health (e.g., pollution), and indirect ones (e.g., by the depletion of the ozone layer). Freight transport in the United Kingdom is responsible for 21% of the CO_2 emissions from the transport sector, amounting to 33.7 million tonnes, or 6% of the CO_2 emissions in the country, of which road transport accounts for a proportion of 92% (McKinnon, 2007). Similar figures apply to the United States, where the percentage of total GHG emissions from transportation rose from 24.9% to 27.3% between 1990 and 2005, with road transport accounting for 78% of the emissions produced by all transportation modes (Ohnishi, 2008). Growing concerns about such hazardous effects of transportation on the environment call for revised planning approaches to road transportation by explicitly accounting for such negative impacts. Our purpose is to introduce a new vehicle routing variant, called the Pollution-Routing Problem (PRP), that will take pollution into account.

The Vehicle Routing Problem (VRP) is central to road transportation planning and aims at routing a fleet of vehicles on a given network to serve a set of customers under side constraints. In the basic version of the problem, all tours start and end at a single depot. The most common variant is the Capacitated VRP (CVRP) where each vehicle is constrained by its capacity on the amount of load it can carry. Another common variant is the VRP with Time Windows (VRPTW) where customers must be visited within predefined time slots. The traditional objectives of the VRP include minimizing the total distance traveled by all vehicles or minimizing the overall travel cost, usually a linear function of distance. The literature on the VRP and its

---

* Corresponding author.
  E-mail addresses: T.Bektas@soton.ac.uk (T. Bektaş), Gilbert.Laporte@cirrelt.ca (G. Laporte).

variants is rich and the reader is referred to the survey by Cordeau et al. (2007) and to the book of Golden et al. (2008) for a recent coverage of the state-of-the-art on models and solution algorithms. It has been suggested by a number of authors (e.g., McKinnon, 2007; Sbihi and Eglese, 2007) that there are opportunities for reducing CO_2 emissions by extending the traditional VRP objectives to account for wider environmental and social impacts rather than just the economic costs.

The amount of pollution emitted by a vehicle depends on load and speed, among other factors. A wide range of models, mainly based on simulation, have been proposed to predict fuel consumption and emission rates such as `aaSIDRA` and `aaMOTION` (Akçelik et al., 2003), the Parametric Analytical Model of Vehicle Energy Consumption (Simpson, 2005), and the Comprehensive Modal Emission Model (Barth et al., 2005), which have been used to test various strategies for CO_2 reduction (e.g., Barth and Boriboonsomsin, 2008). However, from the perspective of minimizing pollution in transportation planning, not much has been done. The PhD dissertation of Palmer (2007) presents an integrated routing and emissions model for freight vehicles and investigates the role of speed in reducing CO_2 emissions under various congestion scenarios and time window settings. The model uses a known VRPTW heuristic as a black-box solver to produce the routing plans within the model. One of the main results is that savings up to 5% in CO_2 emissions can be achieved over time minimizing plans. Palmer (2007) does not, however, account for vehicle loads in his model, although this is offered as a future research topic. Maden et al. (2010) consider a vehicle routing and scheduling problem with time windows in which speed depends on the time of travel. The authors describe a heuristic algorithm to solve the problem and report up to 7% savings in CO_2 emissions by solving a case study involving scheduling of a fleet of delivery vehicles in the United Kingdom. Jabali et al. (2009) consider a similar problem to that of Maden et al. (2010) but estimate the amount of emissions based on a nonlinear function of speed, among other vehicle-specific parameters, and present analyses to find the 'optimal' speed with respect to emissions. The authors make use of an iterative tabu search procedure to solve the problem on instances taken from the VRP literature and study the various costs involved.

Kara et al. (2007) introduce the so-called Energy-Minimizing Vehicle Routing Problem which is an extension of the VRP where a weighted load function (load multiplied by distance), rather than just the distance, is minimized. The authors present a model for this problem, based on a flow formulation of the VRP with a load-based objective function derived from simple physics. The authors provide two illustrative examples illustrating the (rather expected) difference between solutions provided by a load objective and a distance-minimizing function. Their approach, however, does not accurately reflect the actual energy consumed by a vehicle as it fails to account for speed or other technical factors such as the empty vehicle mass, friction, air drag, etc., and therefore does not minimize energy, but only the weighted load carried by the vehicles. Furthermore, there are no time considerations, which, as we will show, play an important role in evaluating costs.

A related study taking into account energy considerations in vehicle routing from a slightly different perspective is due to Hsu et al. (2007). These authors consider a VRP in which perishable food needs to be distributed using vehicles with cold storage equipment. The objective is to minimize a total cost function including transportation, inventory, energy and violations of time windows introduced as soft constraints. The derivation of the energy function is based on the thermal load of a vehicle and is stated as a function of total travel time and time spent in serving customers. It differs in this regard from the one used in the present study.

To our knowledge, the above mentioned studies provide a good, if not exhaustive, coverage of research studies aiming explicity at reducing environmental consequences of vehicle routing. However, similar studies have started appearing in other contexts. For example, Fagerholt et al. (2010) consider the problem of reducing emissions in shipping where the route is predefined and offer an efficient algorithm for this purpose. Bauer et al. (2010) describe an approach to model and minimize emissions in intermodal freight transport and present results on a case study of a rail network operating in Eastern Europe.

This brief survey shows that there is a gap in the literature on the application of energy based models in vehicle routing. Indeed, most studies fail to properly integrate environmental factors, in particular, GHG emissions, and the more traditional operational and economic objectives. In this paper, we aim to fill this gap. In particular, our goal is to: (i) describe an approach to reduce energy requirements of vehicle routing based on a comprehensive emissions model that takes into account a number of factors, including load and speed, (ii) define the PRP as a variant of the VRP, with or without time windows, using a comprehensive objective function which measures and minimizes the cost of GHG emissions along with the operational costs of drivers and fuel consumption, and (iii) perform analyses, using the PRP model and several variants, to shed light on the tradeoffs between various performance measures of vehicle routing, such as distance, load, emissions and costs, assessed through a variety of objective functions. Our focus is on the derivation of insights, as opposed to the more traditional algorithmic and computational performance aspects.

The remainder of the paper is structured as follows. The next section provides a formal description of the problem and the model. Section 3 illustrates the proposed approaches on a sample of problem instances. Mathematical models for the PRP and related problems are derived in Section 4. Computational experimentations and analyses are presented in Section 5. The final section contains our conclusions.

2. Formal description of the Pollution-Routing Problem

The PRP is defined on a complete graph $G = (\mathcal{N}, \mathcal{A})$ with $\mathcal{N} = \{0, 1, 2, \ldots, n\}$ as the set of nodes and $\mathcal{A}$ as the set of arcs defined between each pair of nodes. Node *0* is the depot. There exist a homogeneous set of vehicles $\mathcal{K} = \{1, 2, \ldots, m\}$, each

with capacity Q. The set $\mathcal{N}_0 = \mathcal{N} \setminus \{0\}$ is a customer set and every customer $i \in \mathcal{N}_0$ has demand q_i and a request to be served within a prespecified time interval $[a_i, b_i]$. The time taken by a vehicle to serve customer i is denoted by t_i, and the distance from i to j is denoted by d_{ij}.

Each vehicle emits a certain amount of GHG when traveling over an arc (i,j). This amount is dependent on a number of factors, such as load and speed, among others. Whereas some of these factors are fixed (e.g., gravity and slope), the load and speed variables can be controlled. The load of a vehicle is made up of empty load and carried load. Vehicles (trucks) are usually classified based on their Gross Vehicle Weight Rating (GVWR), which is defined as the maximum allowable total weight of the vehicle including its empty mass, fuel and any load carried. The empty mass of the vehicle (but with fuel and fluids such as engine oil) is termed *curb weight*. Vehicles are usually classified into eight classes with vehicles in the lightest class having a GVWR up to around three tonnes (t), and those in the heaviest class with a GVWR higher than 15 t (Wikipedia, 2009). Our review of a number of different types of vehicles in classes 1, 2, 3 and 4 has revealed that the ratio of the curb weight of a vehicle to its GVWR is 42%, 57%, 48% and 51%, respectively. In practical terms, therefore, it can be concluded that vehicles carry approximately as much cargo as their curb weight.

The speed at which a vehicle travels on arc (i,j) is constrained by a lower bound and an upper bound, denoted l_{ij} and u_{ij}, respectively, usually imposed by traffic regulations. A unit of greenhouse gas emitted (usually in grams) has an estimated cost denoted by e. Such costs are difficult, but not impossible, to quantify. Indeed, there exists a number of published works on the estimation of the social costs of carbon(-dioxide) emissions as well as abatement costs. Forkenbrock (2001)* for instance, reports the cost of CO_2 per ton emitted to be in the range of $10–$20. The paper by Tol (2005) provides an analysis of 133 estimations of marginal CO_2 damage costs gathered from 28 published studies to derive a probability density function. Although he produces statistics based on different criteria (e.g., whether the work is peer-reviewed or not), the main conclusion is that the cost has a mean of $93/t and can be as high as $350/t (in the 95 percentile). In the United Kingdom, the Department of Environment, Food and Rural Affairs (DEFRA, 2007) uses a different measure called the shadow price of carbon and suggests to set it at £27/t of CO_2 emitted for year 2010, and to increase it by 2% for each subsequent year.

Based on these definitions, this paper considers four problems, all of which involve finding a set of tours for the set $\mathcal{K}$ of vehicles that start and end at the depot, such that the total load carried by any vehicle does not exceed its capacity Q. These problems differ with respect to their objective functions, some of which are related to the environment. These objectives are (i) a distance-minimizing objective function assuming constant speed (denoted P_D) which corresponds to the standard CVRP or VRPTW, (ii) a weighted load-minimizing objectve function assuming constant speed (denoted P_L), (iii) an energy-minimizing objective function assuming speed as an endogenous decision (denoted P_E), and (iv) a cost-minimizing objective function encompassing cost of emissions, drivers and fuel (denoted P_C). We discuss below how to account for various types of costs involved in the routing.

2.1. Cost of emissions

The instantaneous engine-out emission rate E in grams per second (g/s) for a GHG (such as CO, HC or NO_x) is directly related to the fuel use rate F (g/s) through the relation $E = \delta_1 F + \delta_2$, where δ_1 and δ_2 are GHG-specific emission index parameters. The calculation of F is complex and depends on a number of factors, for which one may consult the study of Barth et al. (2005, 2009). We work with a simplified exposition of their calculation of F:

$$F \approx (kNV + (P_t/\varepsilon + P_a)/\eta)U, \tag{1}$$

where k is the engine friction factor, N is the engine speed, V is the engine displacement, P_t is the total tractive power demand requirement in watts ($W = kg\ m^2/s^3$) placed on the vehicle, ε is vehicle drivetrain efficiency, P_a is the engine power demand associated with running losses of the engine and additional vehicle accessories (W) such as an air conditioner, $\eta \approx 0.45$ is a measure of efficiency for diesel engines, and U is a value that depends on some constants including N. Parameter P_t is further calculated as follows:

$$P_t = (Mav + Mgv\sin\theta + 0.5C_d A\rho v^3 + MgC_r\cos\theta v), \tag{2}$$

where M is the mass (kg) of the vehicle (empty plus carried load), v is speed (m/s), a is the acceleration (m/s^2), g is the gravitational constant (9.81 m/s^2), θ is the road angle, A is the frontal surface area of the vehicle (m^2), ρ is the air density (kg/m^3), and C_r and C_d are the coefficients of rolling resistance and drag, respectively.

We assume for practical reasons that in a vehicle trip all parameters will remain constant on a given arc (but load and speed may change from one arc to another). In other words, we assume that vehicle will travel at an average speed of $v = v_{ij}$ (meters/sond) on an arc (i,j) with distance d_{ij} (meters) and road angle $\theta = \theta_{ij}$ carrying a total load of $M = w + f_{ij}$, where w is the empty vehicle weight and f_{ij} is the load carried by the vehicle on this arc. The total amount of energy consumed on this arc P_{ij} can then be approximated as:

$$P_{ij} \approx P_t(d_{ij}/v_{ij}) \tag{3}$$
$$\approx \alpha_{ij}(w + f_{ij})d_{ij} \tag{4}$$
$$+ \beta v_{ij}^2 d_{ij}, \tag{5}$$

where $\alpha_{ij} = a + g\sin\theta_{ij} + gC_r\cos\theta_{ij}$ is an arc specific constant, $\beta = 0.5C_dA\rho$ is a vehicle specific constant. We approximate the total amount of energy consumed on a given link (i,j) through relation (3) as opposed to (1) as the parameters required for the latter are vehicle specific and remain constant when a particular vehicle is chosen for a trip. The resulting approximation yields an energy requirement in joules ($J = kg\ m^2/s^2$) which directly translates into fuel consumption and further into GHG emissions. We have purposefully split Eq. (3) into two: (4) representing load-induced energy requirements and (5) corresponding to speed-induced energy requirements, so as to be able to easily refer to these components in the analysis to be presented in Section 3.

The reason behind our choice of this particular emission model is twofold: (i) it is one of the few available models that reflect the change in the vehicle load as it travels, a property that is not available in many of the existing estimation models that assume a static load profile, and (ii) it is also applicable to heavy-duty vehicle emission estimations which apply to freight transportation. This function of emissions per unit distance traveled is typically U-shaped and makes it simple to calculate the optimal speed at which emissions are minimized. We illustrate the behavior of this function in Fig. 1 for a lightweight vehicle. The function has two components, one induced by kNV and shown by the dashed line, and the other mainly by P_t shown by the dotted line. Assuming that a vehicle traverses a leg (i,j) of d_{ij} meters at constant speed v_{ij}, and that all other parameters in function (1) remain the same over this leg, the total estimated fuel consumption will be Fd_{ij}/v_{ij}. Up to a certain level of speed, the contribution of the first component kNV will decrease as speed increases. In contrast, the second component of the function induced by P_t will increase with speed, yielding a U-shaped curve, and an optimal speed of 40 km/h, assuming other parameters are fixed at certain values.

The shape of emission functions such as (1) is very much dependent on a number of factors, including load, resistance and road angle. In any case, the contribution of the first component of the function, namely kNV, will only be significant for very low speed levels (e.g., less than 40 km/h). It is for this reason that the development of our modeling approach will assume speeds of at least 40 km/h and will consider P_t as the primary determinant of the total emission function. This consideration implies that emissions per unit of time (e.g., grams per second) are minimized at the lowest possible speed level for speeds of 40 km/h or higher. In this sense, our approach follows that of Ross (1997) who estimates energy consumption of a vehicle based only on P_t. We believe that environments in which speeds are less than 40 km/h (e.g., congested roads) require a different treatment that offered in this study. We will discuss this further in the last section.

2.2. Operational "en-route" costs

The operational "en-route" costs incurring on each arc $(i,j) \in \mathscr{A}$ traversed by vehicle can simply be calculated as $c_f F_{ij}$, where c_f is the unit cost of fuel and F_{ij} is the fuel consumption over arc (i,j) which is estimated using P_{ij}. One may also incorporate additional running costs into c_f, such as those associated with repairs and maintenance.

2.3. Cost of drivers

The driver of a vehicle is paid at a wage of p per unit time (usually per hour). The total time s that a driver spends on a tour is dependent on the number and the locations of the customers in the tour. The total amount paid to driver can then be expressed as $p \cdot s$.

The next section provides an illustration of the above concepts on a small-size instance.
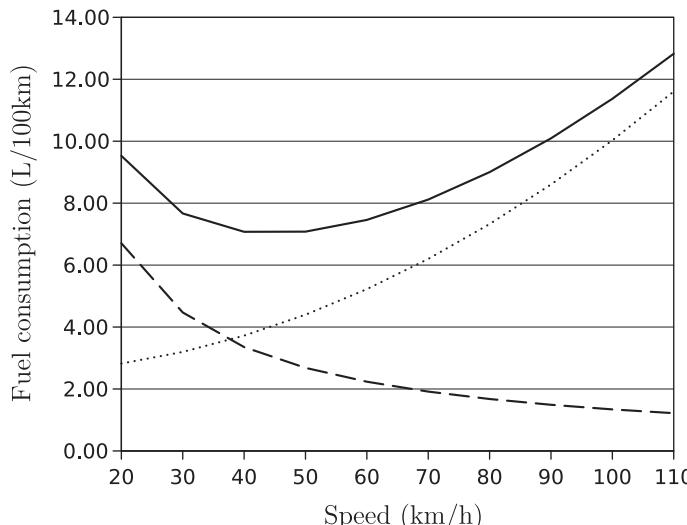

Fig. 1. Fuel consumption as a function of speed, as estimated by function (1).

3. An illustrative example

In this section, we use a four-node instance to show the differences between problems P_D, P_L, P_E and P_C and we also study the effect of speed and time windows on various performance indicators such as distance, energy and cost.

3.1. Distance or load?

We consider the four node network of Fig. 2 represented as a rectangle with the length of each side indicated in kilometers (km), converted from 100 miles for the two short edges and 200 miles for the two long edges (to represent solutions it is convenient to replace each edge with two opposite arcs of equal length). We assume that there is a single uncapacitated vehicle based at node 0 to serve customers 1, 2 and 3. The instance is defined with the following parameters: $C_d = 0.70$, $A = 5.0$ m^2 (both as reported by Akçelik et al. (2003) for a light/medium rigid heavy vehicle), the curb (empty) weight equal to $w = 3$ t, $a = 0$, $\theta_{ij} = 0°$ for all $i,j \in \{0,1,2,3\}$, $i \neq j$, $g = 9.81$ m/s^2 and $\rho = 1.2041$ kg/m^3 (at 20 °C). Speed limitations are set to $l = 40$ km/h and $u = 70$ km/h. The coefficient of rolling resistance C_r is usually between 0.010 and 0.015 for average concrete roads (Genta, 1997, p. 50) and we use $C_r = 0.01$ in our implementation.

If we assume a homogeneous demand pattern as $q_1 = 1$, $q_2 = 1$ and $q_3 = 1$ (in t), no time window restrictions, and allow each vehicle to travel as slowly as possible (here we consider a minimum speed of 40 km/h on each arc), then a distance-minimizing objective P_D yields two optimal tours, (0, 1, 2, 3, 0) and (0, 3, 2, 1, 0) of length 965.61 km. In terms of energy, however, the former tour consumes 192.56 kWh whereas the latter requires 183.79 kWh. Not surprisingly, a weighted load-minimizing objective of P_L (with fixed speed) yields the latter tour as the optimal solution, with a saving of 4.55% in consumption with respect to the former.

3.2. Does speed matter?

Consider now the following example which illustrates that an energy-minimizing objective neglecting speed considerations (i.e., weighted load-minimizing P_L) may yield surprising results. Assume a demand pattern defined as $q_1 = 0.25$, $q_2 = 3.5$ and $q_3 = 0.25$ (in t) with an intentionally very large increase in q_2. In this case, the distance-minimizing objective once again yields the optimal tour (0, 1, 2, 3, 0) with a total energy consumption of 202.42 kWh and a load carrying measure of 4868.27 t km. As above, this objective is independent of customer demands and the tour (0, 3, 2, 1, 0) is also optimal with respect to total distance (965.61 km). In contrast, a weighted load-minimizing objective yields a different tour (0, 2, 1, 3, 0) in which the customer with the heaviest load is visited first. This tour has a length of 1041.60 km and a load carrying measure of 4734.69 t km, which is less than what the distance-minimizing objective yields. However, this tour consumes 204.27 kWh of energy, which is an increase of approximately 1% over that of a distance-minimizing solution. Table 1 provides an insight into this phenomenon. It shows a detailed output of the solutions produced by distance and weighted load-minimizing objectives. This table gives, for each solution, the arc traversed, the load carried on each arc (in t, including the empty weight of the vehicle), the speed at which the vehicle traverses the corresponding arc (in km/h), the partially consumed energy measured by (4), the partially consumed energy measured by (5) and the total energy consumption (in kWh).
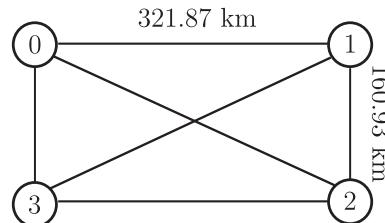
Fig. 2. Sample four-node instance.

Table 1
Comparison of distance and weighted load-minimizing solutions.

Distance-minimizing solution							Weighted load-minimizing solution						
Arc	Load	Distance	Speed	(4)	(5)	Total	Arc	Load	Distance	Speed	(4)	(5)	Total
(0, 1)	3 + 4.00	200.00	40	61.40	23.25	84.65	(0, 2)	3 + 4.00	223.61	40	68.64	26.00	94.64
(1, 2)	3 + 3.75	100.00	40	29.60	11.63	41.23	(2, 1)	3 + 0.50	100.00	40	15.35	11.63	26.98
(2, 3)	3 + 0.25	200.00	40	28.51	23.25	51.76	(1, 3)	3 + 0.25	223.61	40	31.87	26.00	57.87
(3, 0)	3 + 0.00	100.00	40	13.16	11.63	24.78	(3, 0)	3 + 0.00	100.00	40	13.16	11.63	24.78
				132.66	69.76	202.42					129.02	75.25	204.27

Solutions displayed in Table 1 clearly show that, although the weighted load-minimizing solution is indeed able to reduce the load-dependent component (4) of the energy function, it actually increases component (5) because of the increase in traveled distance which is not accounted for in the solution process. Hence, the distance-minimizing solution produces a lower *combined* energy value than the weighted load-minimizing solution, hence yielding a counter-intuitive result that a weighted load-minimizing solution does not necessarily imply the minimization of energy consumption.

An objective that takes into account the complete energy function with speed as a decision variable does make a difference. The solution produced by this objective is (0, 3, 2, 1, 0), where the vehicle travels at 40 km/h on every arc. This solution has a total energy consumption of 200.23 kWh, which represents a 1.08% improvement upon the distance-minimizing solution and a 1.98% improvement upon the weighted load-minimizing solution.

Although such a simple analysis shows the important role played by speed in terms of producing an energy-efficient solution, the savings become even more apparent when time windows are imposed. The subsequent exposition provides more insight into this aspect of the problem.

3.3. Where speed really matters: the effect of time windows

In this section we look at the impact of speed under time windows restrictions and using the sample network in Fig. 2, with $q_1 = 0.1$, $q_2 = 0.5$ and $q_3 = 0.1$ (all in t) with the following time windows (in hours) imposed on nodes: $a_1 = a_2 = a_3 = 0$, $b_1 = 5.5$, $b_2 = 25$ and $b_3 = 17$. We assume that each customer requires 15 minutes of service time. For this instance, a distance-minimizing solution produces an optimal tour (0, 1, 3, 2, 0) due to the time windows restrictions which necessitate going from the depot to node 1 at a speed of 60.98 km/h, proceeding to node 3 at the slowest possible speed of 40 km/h (which does not allow the vehicle to go from node 1 to node 2 since in this case it would not make it to node 3 in time), then to node 2, and back to the depot at the same speed. This solution has a total energy requirement of 257.19 kWh. A weighted load-minimizing solution of P_L without any speed consideration (assuming the lowest possible speed permitted by the time windows) produces the same solution. This is contrary to the expectation that P_L would ensure visiting the second customer as early as possible in the tour (thus dropping the heaviest load as quickly as possible). However, this is not feasible for P_L under the limitations imposed by the time windows since it assumes a fixed speed.

However, under an energy-minimizing objective with speed as a decision variable (i.e., problem P_E), the picture changes. This objective produces an optimal tour (0, 1, 2, 3, 0) whereby the vehicle departs from the depot and travels to node 1 at a speed of 60.98 km/h, then to node 2 at 46 km/h, to node 3 at 42.98 km/h, and finally back to the depot at 40 km/h. Traversing this tour consumes 196.52 kWh of energy with an impressive saving of 23.59% over that of the solution that minimizes either distance or weighted load (without varying speed). It is noteworthy that this solution is in fact infeasible under a scenario that does not consider speed as a decision variable, and feasible under a scenario that does. Comparisons of the solutions produced by distance, load and energy-minimizing objectives are given in Table 2.

These examples clearly demonstrate the potential impacts an energy-minimizing objective function, with load and speed as decision variables, can have in routing. However, they do not tell the whole story in terms of monetary costs. An energy-minimizing solution is of interest only when the amount of CO_2 emissions is of concern. However, there are other cost factors that play a significant role in calculating transportation costs, such as the cost of fuel and the cost of drivers. The former is dependent on the amount of fuel consumed, which is in turn proportional to the amount of energy required to run the vehicle. The latter cost is primarily dependent on the time that a driver spends on the route. We now elaborate further on the cost issue using the above example.

3.4. Cost considerations

In the above discussion, we have only examined the effect of employing different objective functions on distance, weighted load and energy measures and the resulting solutions. We will now show some interesting cost implications of these different solutions. The parameters used for these experiments, in addition to those already defined, are as follows. Energy, once calculated in J and converted into kWh using the conversion one kWh is equal to 3,600,000 J, is translated into fuel requirements using the fact that one L of gasoline is able to provide 8.8 kWh of energy, and gasoline engines have an average fuel (tank-to-wheel) efficiency of 20% (Mima and Criqui, 2003, p. 55; Kreith and West, 2003). We note that the effi-

Table 2
Comparison of distance, load and energy-minimizing solutions.

Distance/weighted load-minimizing solutions							Energy-minimizing solution						
Arc	Load	Distance	Speed	(4)	(5)	Total	Arc	Load	Distance	Speed	(4)	(5)	Total
(0, 1)	3 + 0.70	200.00	60.98	32.45	54.06	86.52	(0, 1)	3 + 0.70	200.00	60.98	32.45	54.06	86.52
(1, 3)	3 + 0.60	223.61	40.00	35.30	26.00	61.30	(1, 2)	3 + 0.60	100.00	46.00	15.79	15.39	31.17
(3, 2)	3 + 0.50	200.00	40.00	30.70	23.25	53.95	(2, 3)	3 + 0.10	200.00	42.94	27.19	26.86	54.05
(2, 0)	3 + 0.00	223.61	40.00	29.42	26.00	55.42	(3, 0)	3 + 0.00	100.00	40.00	13.16	11.63	24.78
				127.87	129.32	257.19					88.59	107.93	196.52

ciency of diesel engines is much higher, being in the range of 32–39% (Mima and Criqui, 2003, p. 55). For the following example, we will use 20% as the engine efficiency, although a higher value of 37% will also be implemented in the computational experiments to account for the effects of advances in engine technology. The cost of fuel is set to £1/L which is an average figure for the United Kingdom (The Automobile Association Limited, 2009). The cost of CO_2 emissions is calculated using the fact that one L of gasoline contains 2.32 kg of CO_2 (Coe, 2005). Hourly wages for vehicle drivers are in the range of £7.80–£8.50 in the United Kingdom (Payscale, 2009a) and of $14.26 to $18.60 in the United States (Payscale, 2009b), depending on a driver's experience. The hourly wage of a driver is therefore set to an average figure of £8.

Considering the settings given in Section 3.2 (i.e., with no time window restrictions and $q_1 = 0.25$, $q_2 = 3.5$ and $q_3 = 0.25$), the cost implications of solving four different problems on the instance are summarized in Table 3. The table presents, for each problem, the break-down of total cost into three components, namely that of CO_2, fuel and drivers.

Table 3 clearly shows the impact of employing different objective functions on a given instance. The results imply that driver cost is the dominant component of the total cost in all cases, followed by the costs of fuel and CO_2 in this order. We note that the weighted load-minimizing objective function (i.e., solution of problem P_L) results in the highest total cost for this specific instance. The optimal solutions of problems P_D and P_E yield similar cost performances. It is also interesting to note that the solution of problem P_C has a higher CO_2 cost, compared to the other three, showing that the emissions are not necessarily minimized. In fact, the solutions to problems P_D, P_L and P_E yield routes in which the vehicle travels at the slowest possible speed of 40 km/h, whereas for P_C the vehicle travels at approximately 52 km/h on each arc with the aim of reducing the driver costs. This solution also yields a higher fuel cost compared to the other three solutions, but despite this fact the overall cost is significantly lower than the rest.

The results of Table 3 were obtained using the cost figure £27/t suggested by DEFRA (2007). In the light of the study by Tol (2005), we have repeated the experiments with 'catastrophic' cost estimates at £60 ($\approx$\$93) and £225 ($\approx$\$350). The results did not change for either of these cases, with the fuel and driver costs staying the same as before. The CO_2 costs for problems P_D, P_L, P_E and P_C turned out to be £16.01, £16.16, £15.84 and £19.64, respectively, for the former case and £60.04, £60.59, £59.39 and £66.06, respectively, for the latter. Even with these increased cost estimates of CO_2, the driver and fuel costs still appear to be the two dominating components of the total cost figure.

3.5. Number and utilization of vehicles

So far we have only considered the single-vehicle case. The use of multiple vehicles will have implications in terms of total fuel consumption, vehicle capacity utilization as well as fixed costs (e.g., rent, amortization). Using a variable number of vehicles as opposed to a fixed one may result in a better utilization of the vehicle capacity. We now look at changes in fuel consumption and capacity utilization in the case of multiple vehicles. When the number of vehicles is a decision variable, the best fleet composition is very much dependent on the fixed vehicle costs, which may vary greatly from one setting to another. It is difficult to estimate such costs as they are dependent on whether the vehicles are company owned or rented on a daily basis. To be able to perform the analysis without the dominating effect of fixed vehicle costs, we predefine three routing plans as shown in Fig. 3. This figure shows, for a set of six customers with equal demand, three cases where (a) three identical vehicles visit two customers each, (b) two identical vehicles visit three customers each, and (c) one vehicle visits all six customers. For this particular example, all pairwise distances are set equal to 10 km each, and all customers have equal

Table 3
Comparison of costs involved in the illustrative example.

| Problem	CO_2	Fuel	Driver	Total
Cost (£)				
P_D	7.20	115.01	199.14	321.36
P_L	7.27	116.06	214.34	337.68
P_E	7.13	113.77	199.14	320.03
P_C	8.84	141.11	154.58	304.53

(a)   **(b)**   **(c)**
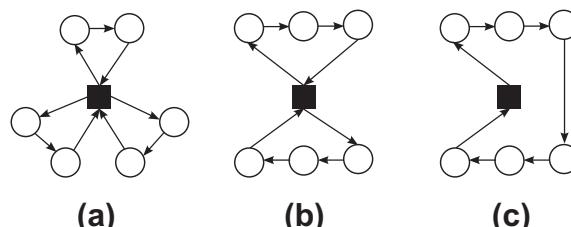
Fig. 3. Network configurations used in the experiments on the number of vehicles and on their utilization.

Table 4
Specification of the 10 scenarios generated for analysing the effect of the number and utilization of vehicles.

Scenarios	1	2	3	4	5	6	7	8	9	10
Vehicle weight (t)	3	3	7	7	7	7	15	15	15	15
Customer demand (each) (t)	0.1	0.5	0.4	0.6	0.8	1.0	0.5	1.0	1.5	2

Table 5
Comparison of fuel consumption and capacity utilization in the case of multiple vehicles.

Scenario	Three vehicles			Two vehicles			One vehicle		
	r_u	40 km/h	60 km/h	r_u	40 km/h	60 km/h	r_u	40 km/h	60 km/h
1	6.67	1.0000	1.0000	10.00	0.8986	0.9000	16.67	0.8174	0.8146
2	33.33	1.0000	1.0000	50.00	0.9396	0.9333	100.00	0.9606	0.9371
3	11.43	1.0000	1.0000	17.14	0.9098	0.9093	34.29	0.8538	0.8481
4	17.14	1.0000	1.0000	25.71	0.9857	0.9185	51.43	0.9529	0.8824
5	22.86	1.0000	1.0000	34.29	0.9297	0.9273	68.57	0.9245	0.9141
6	28.57	1.0000	1.0000	42.86	0.9389	0.9377	85.71	0.9567	0.9456
7	6.67	1.0000	1.0000	10.00	0.9035	0.9024	20.00	0.8268	0.8246
8	13.33	1.0000	1.0000	20.00	0.9145	0.9148	40.00	0.8701	0.8679
9	20.00	1.0000	1.0000	30.00	0.9266	0.9251	60.00	0.9125	0.9080
10	26.67	1.0000	1.0000	40.00	0.9381	0.9372	80.00	0.9525	0.9467

demands. The selection of the latter two sets of parameters are made so that results are comparable. All other parameters are as described previously.

For this experiment, we consider three different vehicle weights, 3 t, 7 t and 15 t, and we generate 10 scenarios as described in Table 4.

Each scenario in Table 4 is run with respect to the three routing plans shown in Fig. 3. For example, under Scenario 1, each customer has 0.1 t demand. For this Scenario, routing plan (a) is where three vehicles of 3 t weight visit two customers each, (b) is where two vehicles of 3 t weight visit three customers each and finally, (c) is where only one vehicle visits all six customers of 0.1 t demand each. Table 5 presents the results of this experiment.

The first column of Table 5 presents the 10 scenarios tested. The columns titled r_u show the utilization ratios (in %) for each vehicle, as calculated by the total amount of goods carried on the vehicle when it starts the tour, over the total empty vehicle weight, which is roughly equal to the total weight capacity of the vehicle. We normalize the total fuel consumption for each scenario to that of the case of three vehicles, and report for each case the results for two different speed levels, one at 40 km/h and the other at 60 km/h. The results presented in Table 5 indicate that in general, the total fuel consumption as estimated by (3) decreases as the number of vehicles is reduced, which also implies an increased utilization ratio. However, there are exceptions as can be seen in the case of the 3 t vehicle with customer demand of 0.5 t, as well as in the case of the 7 t vehicle with 1 t customer demand, where total fuel consumption increases as the number of vehicles decreases from two to one. The main reason for such a change is that the fuel requirements for a single vehicle carrying a significant load serving all customers are higher than total consumption of two vehicles serving the same set of customers, although the utilization ratio for the former is higher than the latter. The ultimate choice of a solution will, however, also depend on vehicle acquisition and drivers' costs.

4. An integer linear programming formulation

The fundamental problem we consider in this paper is formally defined as constructing routes for a set of vehicles to meet the demands of all customers in a way that all vehicles depart from and return to the depot node, no vehicle carries load more than its capacity and each customer is visited within its respective time window. The overall objective is to minimize the total cost that is composed of cost of emissions, operational costs and cost of drivers. We refer to this problem as the Pollution-Routing Problem (PRP).

Our formulation of the problem uses the following decision variables. A binary variable x_{ij} is equal to 1 if a vehicle travels on arc $(i,j) \in \mathscr{A}$. For a given arc $(i,j) \in A$, f_{ij} and v_{ij} respectively represent the amount of commodity flowing and the speed at which a vehicle travels on this arc. Finally, variable y_j represents the time at which service at node $j \in \mathscr{N}_0$ starts.

The natural integer programming formulation of the PRP is nonlinear for two reasons: (i) the energy function (3) contains a speed component v_{ij} which, multiplied by x_{ij}, makes the objective nonlinear, and (ii) the calculation of driver time is also nonlinear (as will be explained below) since it involves multiplying y_j and x_{ij} variables (see Fagerholt et al., 2010 for a similar nonlinearity issue in a related context). We offer below a procedure to linearize both of these nonlinear terms through a discretization of the speed variables v_{ij}.

First, we assume that speed limitations on every arc are the same, i.e., $l_{ij} = l$ and $u_{ij} = u$ for all $(i,j) \in \mathscr{A}$. This assumption is not restrictive and is only introduced for the sake of simplicity in notation. We then define a set of speed levels

$\mathscr{R} = \{1, 2, \ldots, r, \ldots\}$ where each $r \in \mathscr{R}$ for a given arc (i,j) corresponds to a speed interval $[l^r, u^r]$ with $l^1 = l$ and $u^{|\mathscr{R}|} = u$. Consequently, we calculate the "average speed" as $\bar{v}^r = (l^r + u^r)/2$ for each level $r \in \mathscr{R}$. We introduce a new binary variable $z_{ij}^r = 1$ if a vehicle travels at speed level $r \in \mathscr{R}$ on arc (i,j), and 0 otherwise. The new z_{ij}^r and existing x_{ij} binary variables are linked by the following relation,

$$\sum_{r \in \mathscr{R}} z_{ij}^r = x_{ij} \quad \forall (i,j) \in \mathscr{A},$$

which, when combined with the results presented above, yields the following integer *linear* programming formulation of the PRP:

$$\text{Minimize} \quad \sum_{(i,j) \in \mathscr{A}} (c_f + e) \alpha_{ij} d_{ij} w x_{ij} \tag{6}$$

$$+ \sum_{(i,j) \in \mathscr{A}} (c_f + e) \alpha_{ij} f_{ij} d_{ij} \tag{7}$$

$$+ \sum_{(i,j) \in \mathscr{A}} (c_f + e) d_{ij} \beta \left(\sum_{r \in \mathscr{R}} (\bar{v}^r)^2 z_{ij}^r \right) \tag{8}$$

$$+ \sum_{j \in \mathscr{N}_0} p s_j \tag{9}$$

subject to

$$\sum_{j \in \mathscr{N}} x_{0j} = m \tag{10}$$

$$\sum_{j \in \mathscr{N}} x_{ij} = 1 \quad \forall i \in \mathscr{N}_0 \tag{11}$$

$$\sum_{i \in \mathscr{N}} x_{ij} = 1 \quad \forall j \in \mathscr{N}_0 \tag{12}$$

$$\sum_{j \in \mathscr{N}} f_{ji} - \sum_{j \in \mathscr{N}} f_{ij} = q_i \quad \forall i \in \mathscr{N}_0 \tag{13}$$

$$q_j x_{ij} \leqslant f_{ij} \leqslant (Q - q_i) x_{ij} \quad \forall (i,j) \in \mathscr{A} \tag{14}$$

$$y_i - y_j + t_i + \sum_{r \in \mathscr{R}} (d_{ij}/\bar{v}^r) z_{ij}^r \leqslant M_{ij}(1 - x_{ij}) \quad \forall i \in \mathscr{N}, \ j \in \mathscr{N}_0, \ i \neq j \tag{15}$$

$$a_i \leqslant y_i \leqslant b_i \quad \forall i \in \mathscr{N}_0 \tag{16}$$

$$y_j + t_j - s_j + \sum_{r \in \mathscr{R}} (d_{j0}/\bar{v}^r) z_{j0}^r \leqslant L(1 - x_{j0}) \quad \forall j \in \mathscr{N}_0 \tag{17}$$

$$\sum_{r \in \mathscr{R}} z_{ij}^r = x_{ij} \quad \forall (i,j) \in \mathscr{A} \tag{18}$$

$$x_{ij} \in \{0, 1\} \quad \forall (i,j) \in \mathscr{A} \tag{19}$$

$$f_{ij} \geqslant 0 \quad \forall (i,j) \in \mathscr{A} \tag{20}$$

$$z_{ij}^r \in \{0, 1\} \quad \forall (i,j) \in \mathscr{A}, \ r \in \mathscr{R}. \tag{21}$$

The objective function is derived from (3) and contains four components. The first two, (6) and (7), measure the cost incurred by the load carried on the vehicle (including curb weight). Component (8) measures the cost implied by variations in speed. All three of these components translate directly into total cost of fuel consumption and GHG emissions calculated by the unit cost $(c_f + e)$ multiplied by the total amount of fuel consumed over each link (i,j). Finally, the last component (9) measures the total amount paid to the drivers.

Constraints (10) mean that m vehicles depart from the depot. Although the model presently assumes a constant number of vehicles, it is straighforward to extend the model to accommodate a variable number of vehicles by treating m as a decision variable and augmenting the objective function (6) by a component ξm where ξ corresponds to the unit vehicle acquisition cost. Constraints (11) and (12) guarantee that each customer is visited exactly once. Balance of flow is described through constraints (13) which model the flow as increasing by the amount of demand of each visited customer. Constraints (14) are used to restrict the total load a vehicle carries by its capacity. Time windows are imposed by constraints (15), which are obtained through a linearization of a set of nonlinear inequalities, as in Cordeau et al. (2007) with $M_{ij} = \max\{0, b_i + s_i + d_{ij}/l_{ij} - a_j\}$, and by constraints (16).

The total driving time for each vehicle is dependent on the last node visited in the corresponding tour (i.e., a node j for which $x_{j0} = 1$). Since node j would be visited at time y_j by a driver, the total time required for the corresponding tour would be $y_j + t_j + d_{j0}/v_{j0}$. Based on these arguments, we denote by s_j the total time spent on a route that has node $j \in \mathscr{N}_0$ as last visited before returning to the depot and calculate it as follows:

$$s_j = (y_j + t_j + d_{j0}/v_{j0}) x_{j0}. \tag{22}$$

Constraints (17) are linearizations of Eq. (22) used to calculate the total driving time for each vehicle where L is a sufficiently large number. As was defined in Section 2, t_j denotes the service time for customer $j \in \mathcal{N}_0$.

Formulation (6)–(21) is valid for the PRP and is denoted by F_C. The three remaining problems P_D, P_L, P_E discussed above can now be derived as variations of F_C as follows:

1. A model for P_D with a distance-minimizing objective function is

$$\text{Minimize} \quad \sum_{(i,j)\in\mathscr{A}} d_{ij}x_{ij},$$

subject to constraints (10)–(14),

$$y_i - y_j + t_i + T_{ij} \leqslant M_{ij}(1 - x_{ij}) \quad \forall i,j \in \mathcal{N}_0, \ i\neq j \tag{23}$$

$$a_i \leqslant y_i \leqslant b_i \quad \forall i \in \mathcal{N}_0 \tag{24}$$

$$y_j + t_j + T_{j0} - s_j \leqslant L(1 - x_{j0}) \quad \forall j \in \mathcal{N}_0, \tag{25}$$

and (19)–(21), where T_{ij} is the time spent while traveling from node i to node j (which we will discuss below in more detail). This model is denoted F_D.

2. A model for P_L with a weighted load-minimizing objective function is

$$\text{Minimize} \quad \sum_{(i,j)\in\mathscr{A}} \alpha_{ij}d_{ij}wx_{ij} + \sum_{(i,j)\in\mathscr{A}} \alpha_{ij}f_{ij}d_{ij}, \tag{26}$$

subject to constraints (10)–(14), (23)–(25), (19)–(21) and denoted F_L.

3. A model for P_E with an energy-minimizing objective function is

$$\text{Minimize} \quad \sum_{(i,j)\in\mathscr{A}} \alpha_{ij}d_{ij}wx_{ij} + \sum_{(i,j)\in\mathscr{A}} \alpha_{ij}f_{ij}d_{ij} + \sum_{(i,j)\in\mathscr{A}} d_{ij}\beta\left(\sum_{r\in\mathscr{R}}(\bar{v}^r)^2 z_{ij}^r\right),$$

subject to constraints (6)–(21) and denoted F_E. We note that this model is only valid beyond a certain speed level, e.g., at least 40 km/h, due to reasons discussed in Section 2.1. If lower speeds need to be taken into account (e.g., in case of congestion), then the objective function should be augmented with the kNV component of the emission function (1) along the similar lines of our approach.

Each of the four models above can be defined with or without the time window constraints. In the latter case, constraints (23)–(25) are removed from formulations F_D and F_L, and constraints (15)–(17) are removed from formulation F_E, and constraints (16) are removed from formulation F_C.

4.1. Post-processing of speed for F_D and F_L

Models F_D and F_L require fixed inputs for the T_{ij} values in order to write constraints (23)–(25) However, since speed decisions are exogenous variables to both models, one would have to set these values a priori, which may cause problems. In our implementation, we use the following strategy to deal with this issue. The T_{ij} values are tentatively set, for each arc $(i,j) \in A$, equal to $T_{ij} = d_{ij}/v^{r^*}$, where $r^* = \text{argmin}_{r\in\mathscr{R}}\{a_i + t_i + d_{ij}/\bar{v}^r \leqslant b_j\}$ before the optimization. This calculation actually results in a lower bound relying on the slowest possible speed at which a vehicle needs to traverse an arc (i,j) so that time windows are not violated. The assumption made is that the vehicle will reach node $i \in \mathcal{N}_0$ exactly at time a_i. Even though constraints might yield a feasible solution to the model, they may be infeasible for the problem if the actual arrival time y_i at node i is larger than a_i. An example of this situation is given in Fig. 4 in which an arc (i,j) is to be traversed where $a_i = 10$, $b_i = 30$ and $a_j = 60$, $b_j = 65$ and there are three discretized speed levels as $\bar{v}_1 = 15$ m/s, $\bar{v}_2 = 20$ m/s and $\bar{v}_3 = 25$ m/s. We assume no service times for this specific example. Assuming the vehicle will arrive at node i exactly at time 10, T_{ij} would have to be set at $1000/20 = 50$ at constant speed $\bar{v}_2 = 20$ m/s (since neither $\bar{v}_1$ nor $\bar{v}_3$ would be feasible). However if the actual arrival time at node i turns out to be 20, which is feasible for the problem (but not the model as the arrival time at node j), then the speed would have to be increased to 25 m/s for the time window of node j to be respected. However, since speed is an exogenous variable for models F_D and F_L, the change cannot be done during the optimization and would have to be implemented after an optimal solution has been found.

To fix this problem, we employ the methodology used by Fagerholt et al. (2010) for optimizing speed on a fixed route which is based on discretizing the time windows and solving a minimum cost path problem on an augmented network.

[10, 30]   1000 m   [60, 65]
   i ─────────────────────────────── j
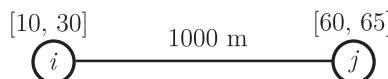
Fig. 4. An example for post-optimization of speed.

An alternative way of calculating the tentative travel times would be to set them equal to $T_{ij} = d_{ij}/v^{r^*}$, where $r^* = \mathrm{argmin}_{r \in \mathcal{R}}\{b_i + t_i + d_{ij}/z_{ij}^r \leqslant b_j\}$. However this may overconstrain the problem as it assumes a worst-case scenario where node i is reached at time b_i and thus some feasible arcs will become infeasible even before solving the model. As a result, we did not choose to implement this strategy.

4.2. Strengthening the PRP formulation

Our preliminary experiments have shown that solving formulation F_C requires a substantial amount of computer time on instances involving only 10 nodes, especially for the case where no time window constraints are imposed. To reduce the solution time, we use the liftings of the bounding constraints (24) as presented in Cordeau et al. (2007) (following Desrochers and Laporte, 1991) and we adapt them to the PRP as follows:

$$y_i - \sum_{j \in \mathcal{N}} \sum_{r \in \mathcal{R}} \max\{0, a_j - a_i + t_j + d_{ji}/\bar{v}^r\} z_{ji}^r \geqslant a_i \quad \forall i \in \mathcal{N}_0$$

$$y_i + \sum_{j \in \mathcal{N}} \sum_{r \in \mathcal{R}} \max\{0, b_i - b_j + t_i + d_{ij}/\bar{v}^r\} z_{ij}^r \leqslant b_i \quad \forall i \in \mathcal{N}_0.$$

We also supplement the formulation with two-node subtour breaking constraints $x_{ij} + x_{ji} \leqslant 1, \forall i, j \in \mathcal{N}_0$. A three-node variation of these constraints has not been used, however, as preliminary experimentations have not shown any significant benefits resulting from these constraints.

5. Computational analysis

Experiments were run with data generated as realistically as possible. Three classes of problems with 10, 15 and 20 cities were generated, where each class includes 10 instances and nodes represent United Kingdom cities. All experiments were performed with a single vehicle having a curb weight of three tonnes (implying it could carry goods weighing approximately the same amount). Whereas our model can handle multiple vehicles, we only consider the single-vehicle case in the analyses since any savings obtained with one vehicle translate into similar savings for several vehicles. Analyses were carried out for cases where customer demands are initially generated randomly according to a discrete uniform distribution on the interval [130, 150], and there are no time windows. However, further analyses were conducted to study the effects of variance in demand, of vehicle type and of time windows. In the experiments, we have used 10 points for discretization. Settings for all other parameters (e.g., speed limitations, costs, energy conversion) are presented in Section 3.

All experiments were conducted on a server with 3 GHz speed and 1Gb RAM. We used CPLEX 12.1 with its default settings as the optimizer to solve the integer linear programming models and the solver was allowed to run its branch-and-cut in a parallel mode (up to four threads) to accelerate the solution process. A common time-limit of three hours was imposed on the solution time of all instances.

5.1. Results for instances without time window constraints

This section presents the results of analyses without time window constraints, using the four different formulations. Table 6 presents the four following measures obtained by the four formulations: total travelled distance (D), total weighted load (LD), total time spent on route including travel and delivery (TT), and total energy consumed (E). All values are standardized to one for the F_D objective and are averaged across 10 instances in each class. Each table is presented with two different levels of engine efficiency, one at 20% and the other at 37%.

Some interesting implications of the results presented in Table 6 are as follows. Both F_L and F_E require slightly more time and distance than F_D to complete the tour but yield less energy consumption, with savings up to 2%. In contrast, both formulations yield shorter trip time requirements and less cumulative load. In comparison, F_L and F_E yield somewhat similar

Table 6
Results of experiments without time windows on distance, load, travel time and energy.

n	F_L				F_E				F_C			
	D	LD	TT	E	D	LD	TT	E	D	LD	TT	E
At 20% efficiency												
10	1.0046	0.9914	1.0037	0.9970	1.0012	0.9926	1.0010	0.9962	1.0000	0.9956	0.8923	1.1343
15	1.0046	0.9627	1.0036	0.9793	1.0046	0.9627	1.0036	0.9793	1.0005	0.9673	0.8981	1.1086
20	1.0081	0.9767	1.0062	0.9887	1.0013	0.9774	1.0011	0.9865	1.0009	0.9821	0.9017	1.1125
At 37% efficiency												
10	1.0046	0.9914	1.0037	0.9970	1.0012	0.9926	1.0010	0.9962	1.0000	0.9956	0.7436	1.4653
15	1.0046	0.9627	1.0036	0.9793	1.0046	0.9627	1.0036	0.9793	1.0000	0.9674	0.7566	1.4181
20	1.0081	0.9767	1.0062	0.9887	1.0013	0.9774	1.0011	0.9865	1.0009	0.9820	0.7652	1.4104

results in terms of energy consumption but there are instances in which the energy requirements obtained with F_E are less than those obtained with F_L. The change in engine efficiency levels does not alter the values of F_L and F_E. Figs. 5–7 show tour maps obtained by the four formulations for a sample 10-node instance.

Fig. 5 shows a distance-minimizing tour of length 455.77 km and consuming approximately 89.71 kWh of energy visiting the cities of Stoke-on-Trent, Derby, Eastwood, Mansfield, Sheffield, Stockport, Preston, Liverpool, Chichester and Warrington in this order. The vehicle speed is 40 km/h throughout this route. Fig. 6, on the other hand, shows a weighted load-minimizing tour of length 504.53 km and consuming approximately 88.42 kWh of energy, successively visiting the cities of Stoke-on-Trent, Stockport, Preston, Liverpool, Chester, Warrington, Sheffield, Mansfield, Eastwood and Derby. The vehicle travels at 40 km/h throughout this route. Finally, Fig. 7 illustrates an energy-minimizing tour of length 464.13 km and consuming approximately 87.56 kWh of energy, successively visiting the cities of Stoke-on-Trent, Warrington, Preston, Liverpool, Chester, Stockport, Sheffield, Mansfield, Eastwood and Derby. The vehicle travels at 40 km/h throughout this route. We note that the tour shown in Fig. 7 is also cost-minimizing when the vehicle travels at 52 km/h.

F_C has a performance very similar to F_D in terms of total distance, but yields significantly shorter travel times and more energy consumption. There is more energy consumption at 37% efficiency than at 20%, but the trip times are shorter. The
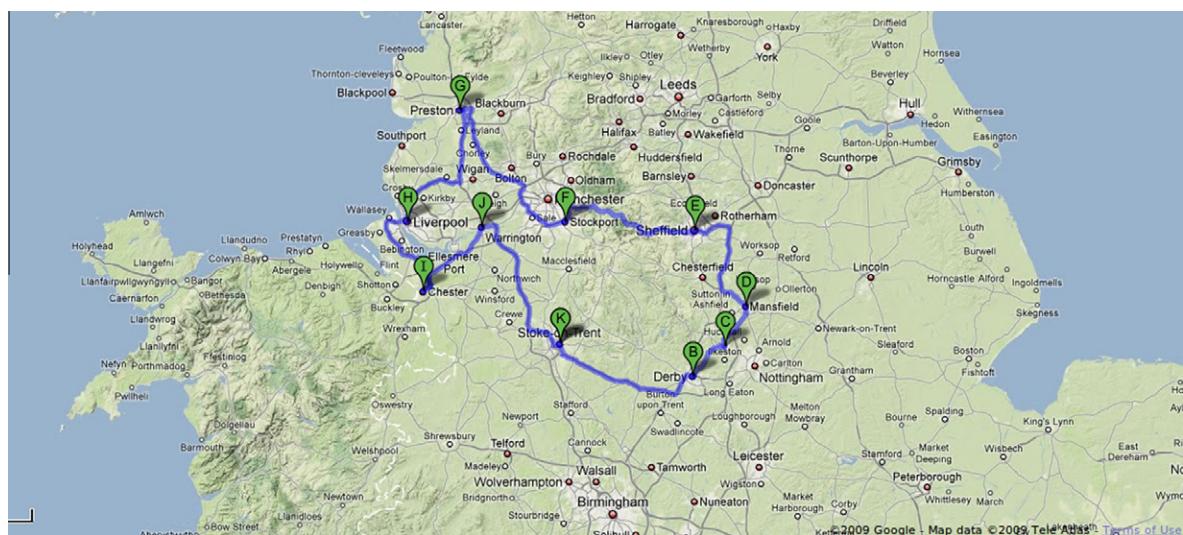

Fig. 5. A distance-minimizing tour.
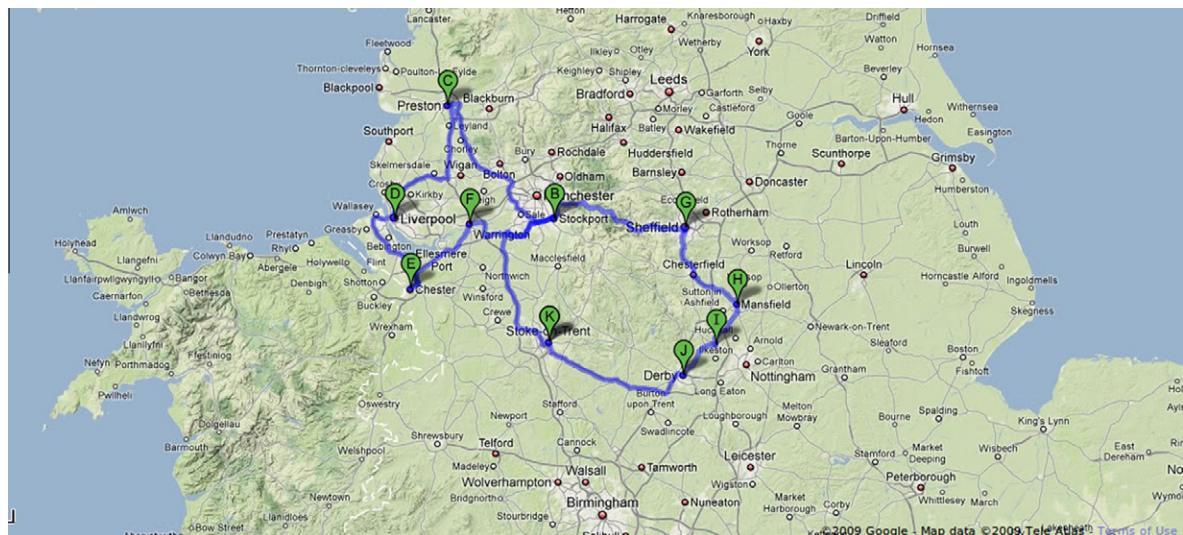

Fig. 6. A weighted load-minimizing tour.
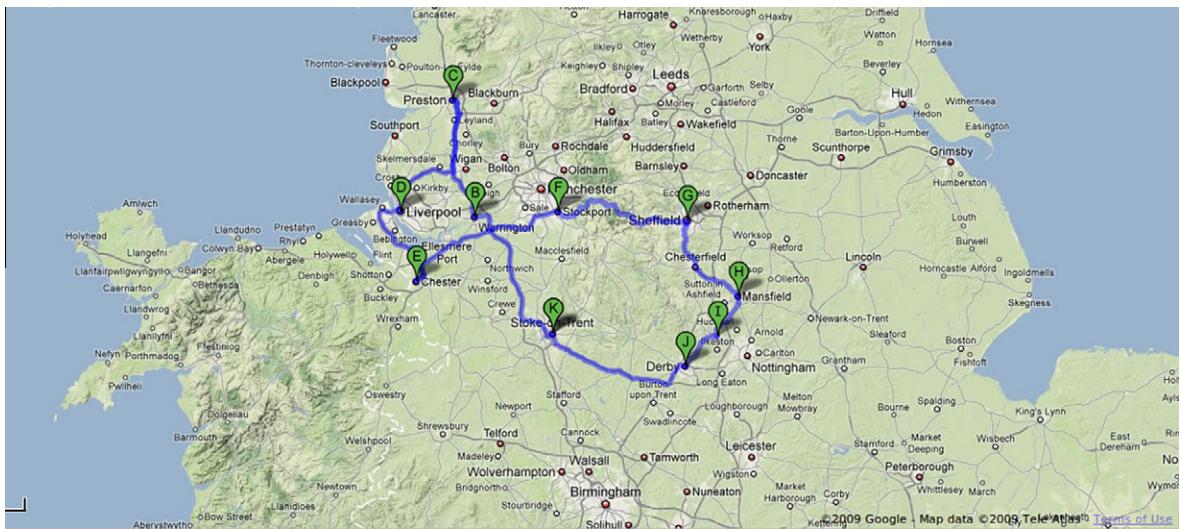
Fig. 7. An energy and cost-minimizing tour.

Table 7
Results of experiments without time windows on various cost measures.

n	F_L				F_E				F_C			
	CO_2	Fuel	Driver	Total	CO_2	Fuel	Driver	Total	CO_2	Fuel	Driver	Total
At 20% efficiency												
10	0.9970	0.9970	1.0038	1.0012	0.9963	0.9963	1.0010	0.9992	1.1343	1.1343	0.8923	0.9829
15	0.9794	0.9793	1.0036	0.9944	0.9794	0.9794	1.0036	0.9945	1.1086	1.1086	0.8981	0.9777
20	0.9887	0.9886	1.0061	0.9995	0.9865	0.9865	1.0010	0.9955	1.1125	1.1125	0.9017	0.9817
At 37% efficiency												
10	0.9970	0.9970	1.0038	1.0021	0.9962	0.9962	1.0010	0.9999	1.4653	1.4654	0.7437	0.9201
15	0.9794	0.9793	1.0036	0.9976	0.9794	0.9793	1.0036	0.9976	1.4181	1.4181	0.7566	0.9201
20	0.9886	0.9887	1.0061	1.0018	0.9865	0.9866	1.0010	0.9974	1.4104	1.4104	0.7651	0.9253

reason for this phenomenon is not obvious from Table 6 but is explained by the cost-driven objective function of F_C. Therefore, to shed more light on this issue, we present the cost implications of these results in Table 7.

The figures shown in Table 7 make it clear that F_C results in more fuel consumption, hence more CO_2 emissions. This objective reduces the trip times by traveling at higher speeds, which is the reason behind the 10–13% increase in fuel and CO_2 costs at 20% engine efficiency, and for the even higher increase (around 45%) at the 37% efficiency level. Although this seems a significant increase in the operational costs, these results correspond to an overall cost reduction of 2–3% at the lower efficiency level, and of around 7–8% at the higher efficiency level. These figures in turn imply that driver wages play a significant role in the overall cost and are relatively more important than fuel or emission costs. This is why the tours resulting from F_C consume more energy by traveling faster, but while doing so they bring down the driver costs. The results also show that, with the proposed approach, reductions of up to 11% (at a low engine efficiency level) and up to 25% (at a high engine efficiency level) in driver costs are possible.

Both F_L and F_E perform better than F_D in terms of fuel and emission costs, although there are instances, where the latter objective results in a smaller total cost than the former two (n = 10 at 20% efficiency and n = 10, 30 at 37% efficiency). It is also interesting to note that F_L may yield, at times, higher overall costs than F_D, suggesting that the two objectives, one driven by load and the other by distance, potentially yield different tours and hence different overall costs. This does not seem to be the case for F_E. An interesting conclusion to be made here is that even in the light of technological advances to improve engine efficiencies, operational (driver) costs still seem to be the dominating cost component. More specifically, at a 20% efficiency level, driver costs make up 65% of the total cost both for F_L and F_E on average, and 57% for F_C on average for the instances tested here. The same figures at a 37% efficiency level are, on average 76% and 62%, respectively. In the rest of the analysis, we work with a 20% efficiency level assuming vehicle runs on a gasoline engine.

The routes that appear as a result of the experiments presented here are of reasonable length and duration. However, when there are more customers in the data set or service time requirements are greater, the solutions may result in routes with extensive length requiring the use of overtime labor. Overtime labor is expensive and would significantly increase the

overall cost. To avoid such outcomes, one can set a strict limit on route duration and ensure the vehicle fleet is able to serve the customers within the imposed limits. Another approach is to allow for overtime (as was done, for example, by Cornillier et al., 2009). In the VRP literature, by far the most common convention is to work with bounded route durations. Both approaches can be easily reflected on the proposed model.

Although the focus of this paper is not on the algorithmic aspects of the PRP, we will briefly mention here, as a side note, the computational performances of the four models. For the 10-node instances, F_D, F_L and F_E all required no more than two seconds of CPU time, whereas the corresponding figure for F_C was 3165.85 CPU seconds, with all instances solved to optimality. The average solution times for the 15-node instances were on average less than three CPU seconds for the first three models. As for F_C, none of the 15-node instances were solved to optimality within the imposed time-limit of three hours. Finally, for 20-node instances, the average solution time requirements were 0.85, 3555.5 and 924.05 CPU seconds for F_D, F_L and F_E, respectively, with a single instance not solved to optimality by F_L. In this respect, it is interesting to note that although F_L and F_E yield somewhat similar solutions, the latter seems to be much more easily solved than the former. As for F_C, none of the 20-node instances was solved to optimality within the imposed time limit. The corresponding figures for F_C presented in Tables 6 and 7, and those presented in what follows, are therefore not optimal. However, when we look closer at the optimization of the 15 and 20-node instances, we see that F_C finds the optimal solution early in the optimization phase and spends the rest of the time trying to improve the lower bound to prove optimality.

5.2. Effect of time windows

This section presents the results of computational experiments where time window constraints are in place. For this purpose, we use the distance data of a single 10-node instance. Time windows are initially introduced to be quite loose; more specifically they are chosen as randomly selected intervals of about 90% of the total time required to complete the full tour. From this instance, three nodes are then randomly selected and their demands are perturbed by a multiplicative factor while simultaneously narrowing down the corresponding time windows by a factor of γ set in the range of 20–60% in increments of 10%. The instances are selected in a way to ensure that (i) the ratio of the load carried by of the vehicle to its GVWR is at most around 1.0, and (ii) the time windows are sufficiently tight to allow for speed variations, but not tight enough to render the instance infeasible. Results of this experiment are presented in Table 8 where each row of the table presents averages across 10 randomly produced instances.

The results shown in Table 8 indicate that savings in energy consumption with F_E can be as high as 10% over the traditional distance-minimizing objective. This is significantly higher than the case without the time window constraints. When time windows are very narrow, however, there is no significant difference in the solutions yielded by formulations F_D, F_L or F_E. The reason is that the tightness of the time windows under a single vehicle scenario almost dictates an optimal route and overrestricts the search space by cutting off many alternative solutions. Another interesting observation is that, under time window constraints, the opportunities for energy reduction become more apparent, especially when comparing F_L and F_E. For cases where time windows are narrowed-down by 20% and 30%, there is a noticeable difference between the energy reductions yielded by both formulations, which is in contrast to cases where time window constraints are not in place. In particular, F_E achieves an energy reduction of up to 10% under a 20% narrowing-down scenario, whereas the savings achieved by F_L is around 5%. Under a 30% narrowing scenario, the respective figures are 6.6% versus 0.03%. Furthermore, in some cases, F_L may result in tours with a higher energy consumption than those produced by F_D, as can be seen in the case of a 50% narrowing-down scenario. We also note that there were instances where tightened time windows with $\gamma \geqslant 80\%$ which did not permit finding a feasible solution for models F_D and F_L (due to some arcs becoming infeasible), whereas in contrast F_E and F_C were able to find feasible solutions for the same instances due to their flexibility in adjusting speed during the optimization phase. The cost implications of the results presented in Table 8 are shown in Table 9.

The results shown in Table 9 suggest that significant cost reductions in CO_2 emissions and fuel costs of up to 12% are possible using model F_E compared to those produced by either F_D and F_L. This, however, comes at the expense of increased driver costs. In general, models F_D, F_L and F_E do not yield significant reductions in total costs. On the other hand, F_C implies a reduction of around 5% in total cost in spite of the increases in emission and fuel costs. Of notable importance, F_C yields reductions in driver costs that go as high as 20%.

Table 8
Results of the experiments with time window constraints.

γ (%)	F_L				F_E				F_C			
	D	LD	TT	E	D	LD	TT	E	D	LD	TT	E
20	1.0107	0.9659	1.0386	0.9492	1.0000	0.9713	1.0656	0.8995	1.0000	0.9894	0.8744	1.1288
30	1.0107	0.9306	0.9846	0.9969	1.0000	0.9346	1.0203	0.9340	1.0000	0.9467	0.8168	1.1911
40	1.0000	1.0000	1.0000	1.0000	1.0000	1.0000	1.0000	1.0000	1.0000	0.9911	0.7954	1.2715
50	1.0157	0.9982	1.0145	1.0055	1.0000	1.0000	1.0000	1.0000	1.0017	1.0145	0.7929	1.2929
60	1.0000	1.0000	1.0000	1.0000	1.0000	1.0000	1.0000	1.0000	1.0019	1.0016	0.8023	1.2671

Table 9
Cost results of the experiments with time window constraints.

γ (%)	F_L				F_E				F_C			
	CO_2	Fuel	Driver	Total	CO_2	Fuel	Driver	Total	CO_2	Fuel	Driver	Total
20	0.9420	0.9422	1.0314	0.9989	0.8881	0.8882	1.0734	1.0059	1.1143	1.1144	0.8848	0.9685
30	1.0142	1.0142	0.9707	0.9856	0.9438	0.9436	1.0100	0.9872	1.2025	1.2024	0.8099	0.9448
40	0.9963	0.9964	1.0184	1.0109	0.9718	0.9718	1.0207	1.0040	1.2333	1.2331	0.8125	0.9563
50	1.0055	1.0055	1.0145	1.0116	1.0000	1.0000	1.0000	1.0000	1.2928	1.2929	0.7928	0.9557
60	1.0000	1.0000	1.0000	1.0000	1.0000	1.0000	1.0000	1.0000	1.2671	1.2671	0.8023	0.9535

5.3. Effect of the variation in demand

The example shown in Section 3 presents cases where the effect of the variation in demand on various measures (e.g., emissions, cost) is significant. This section presents results of further analyses designed to provide a fuller assessment of the demand variation. To this end, using a single 10-node instance, we have performed additional experiments in which the demands are relatively small and smooth. We then gradually performed perturbations on a randomly chosen subset of nodes.

The amount of perturbation is performed by applying a multiplicative constant to three and five randomly selected nodes in such a way that the standard deviation of the set of demands (denoted σ) steadily increases. Averages of the results calculated across 10 instances are given in Table 10 below.

The results presented in Table 10 suggest that the potential reduction in energy consumption becomes higher as the variation between customer demands (represented by the standard deviation in our case) increases. This is even more so in the case where there are relatively fewer nodes having a high demand, rather than a large number of nodes with a high demand, hence supporting the assertion made in Section 3 using the example. These results also show that F_L and F_E do not necessarily yield similar results when the variance in demand grows larger.

We do not present here the associated cost figures for the results presented in Table 10 since they are not much different from those of Table 7, and the effect of variation in demands has a more significant effect on energy consumption than on cost.

5.4. Effect of vehicle type, empty load and carried load

This section looks at the implications of using different vehicles (specified by their corresponding GVWR) and the maximum amount of load carried on the vehicle on the performance measures. To this end, we have conducted experiments using three types of vehicles with respective empty loads of three, five and nine tonnes. The individual demands were then increased uniformly, all by the same multiplier, in such a way that the ratio of the total carried load to the vehicle's curb weight (denoted ω) is at the following three levels: low ($0.25 \leqslant \omega \leqslant 0.35$), medium ($0.50 \leqslant \omega \leqslant 0.60$) and high ($0.85 \leqslant \omega \leqslant 0.95$). The experiments were conducted on the 10-node instances only and average results collected over 10 instances are reported in Table 11 on the four measures of performance.

The figures shown in Table 11 suggest that the variations in the results do not change much from one vehicle type to the other, but the general behavior with varying ω is the same for each type. The implication is that as the vehicle load becomes larger, the potential savings in energy consumption increases. An interesting case is with the nine-tonne vehicle and $\omega = 0.86$, where the solution output by F_C is remarkably close to that of F_D in terms of energy but requires less time and fuel consumption, hence costs less.

Table 10
Results showing the effect of the variation in demand.

σ	F_L				F_E				F_C			
	D	LD	TT	E	D	LD	TT	E	D	LD	TT	E
Three randomly selected nodes												
61.46	1.0000	0.9941	1.0000	0.9967	1.0000	0.9941	1.0000	0.9967	1.0000	1.0058	0.7890	1.3057
106.60	1.0000	0.9825	1.0000	0.9901	1.0000	0.9825	1.0000	0.9901	1.0000	1.0062	0.7886	1.3010
233.87	1.0000	0.9605	1.0000	0.9769	1.0000	0.9605	1.0000	0.9769	1.0031	0.9718	0.7874	1.2769
492.96	1.0520	0.9291	1.0481	0.9764	1.0031	0.9381	1.0029	0.9631	1.0000	0.9455	0.7873	1.2318
Five randomly selected nodes												
66.31	1.0000	1.0000	1.0000	1.0000	1.0000	1.0000	1.0000	1.0000	1.0017	1.0377	0.7885	1.3237
130.95	1.0000	0.9966	1.0000	0.9980	1.0000	0.9966	1.0000	0.9980	1.0017	1.0159	0.7885	1.2981
288.20	1.0111	0.9754	1.0102	0.9901	1.0000	0.9774	1.0000	0.9867	1.0000	1.0314	0.7873	1.3018
529.81	1.0421	0.9694	1.0389	0.9980	1.0017	0.9755	1.0016	0.9858	1.0017	0.9755	0.7908	1.2546

Table 11
Results showing the effect of the amount of goods carried and the vehicle type.

ω	F_L				F_E				F_C			
	D	LD	TT	E	D	LD	TT	E	D	LD	TT	E
w = 3 t												
0.34	1.0043	0.9832	1.0035	0.9922	1.0012	0.9836	1.0010	0.9912	1.0000	0.9874	0.8118	1.2858
0.51	1.0046	0.9824	1.0037	0.9916	1.0025	0.9833	1.0020	0.9912	1.0003	0.9891	0.8095	1.2800
0.93	1.0076	0.9584	1.0062	0.9769	1.0046	0.9591	1.0037	0.9762	1.0018	0.9694	0.8105	1.2413
w = 5 t												
0.28	1.0025	0.9885	1.0020	0.9929	1.0012	0.9886	1.0010	0.9926	1.0000	0.9906	0.8094	1.2128
0.58	1.0052	0.9843	1.0042	0.9904	1.0049	0.9845	1.0039	0.9904	1.0016	0.9916	0.8112	1.1967
0.89	1.0076	0.9720	1.0062	0.9817	1.0046	0.9726	1.0037	0.9813	1.0043	0.9729	0.8120	1.1689
w = 9 t												
0.28	1.0025	0.9935	1.0020	0.9954	1.0012	0.9936	1.0010	0.9952	1.0016	0.9951	0.8104	1.1389
0.58	1.0046	0.9708	1.0037	0.9771	1.0046	0.9708	1.0037	0.9771	1.0012	0.9733	0.8101	1.1066
0.86	1.0076	0.9642	1.0062	0.9717	1.0064	0.9644	1.0052	0.9716	1.0046	0.9647	0.8122	1.0901

As in Section 5.3, we do not present the cost results to the solutions in Table 11 since they are not very different from those of Table 9.

5.5. Effect of a variable number of vehicles

The analysis presented so far considered the routing of a single vehicle. In this section, we present results of computational experiments to analyze the effects of using multiple vehicles. In particular, we consider two alternatives where (i) the number of vehicles is fixed, and (ii) the number of vehicles is variable and each vehicle has a fixed acquisition cost. As for the former case, we carry out experiments with 10, 15 and 20-node instances with time-windows and consider the use of two and three vehicles. The results of this experiment are presented in Table 12 showing the effects on non-financial measures, and in Table 13 for cost measures. Each row in both tables presents averages of ten instances.

The results shown in Tables 12 and 13 are similar to those shown for the single-vehicle case as far as the relative performance of the different models is concerned. This observation indicates that other conclusions drawn for the latter directly translate into the multiple vehicle case. However, some other interesting results can be drawn from Table 13 relative to the use of multiple vehicles. Given a fixed number of vehicles, the results show that cost savings decrease as instances get larger.

Table 12
Effects of the use of multiple vehicles on distance, load, travel time and energy.

n	F_L				F_E				F_C			
	D	LD	TT	E	D	LD	TT	E	D	LD	TT	E
Two vehicles												
10	1.0079	0.9730	1.0285	0.9886	1.0033	0.9736	1.0186	0.9863	1.0254	1.0316	0.7894	1.2869
15	1.0313	0.9289	1.0662	0.9703	1.0098	0.9406	1.0439	0.9684	1.0557	1.0371	0.8799	1.2865
20	1.0350	0.9090	1.0350	0.9574	1.0204	0.9203	1.0452	0.9586	1.1050	1.0212	0.9562	1.1917
Three vehicles												
10	1.0024	0.9890	1.0335	0.9956	1.0014	0.9895	1.0286	0.9947	1.0383	1.0365	0.8116	1.2932
15	1.0245	0.9751	1.0320	0.9958	1.0101	0.9772	1.0173	0.9909	1.0703	1.0788	0.8377	1.3038
20	1.0393	0.9156	1.0372	0.9643	1.0178	0.9206	1.0263	0.9587	1.1388	1.0400	0.9321	1.2457

Table 13
Effects of the use of multiple vehicles on various cost measures.

n	F_L				F_E				F_C			
	CO_2	Fuel	Driver	Total	CO_2	Fuel	Driver	Total	CO_2	Fue l	Driver	Total
Two vehicles												
10	0.9883	0.9887	1.0285	1.0180	0.9861	0.9863	1.0186	1.0097	1.2877	1.2870	0.7894	0.9168
15	0.9704	0.9703	1.0661	1.0405	0.9688	0.9684	1.0439	1.0235	1.2868	1.2865	0.8799	0.9859
20	0.9571	0.9574	1.0349	1.0142	0.9587	0.9568	1.0450	1.0219	1.0381	1.0387	0.9759	0.9938
Three vehicles												
10	0.9958	0.9956	1.0336	1.0246	0.9952	0.9947	1.0287	1.0206	1.2934	1.2932	0.8116	0.9292
15	0.9958	0.9958	1.0319	1.0227	0.9909	0.9909	1.0173	1.0104	1.3035	1.3038	0.8378	0.9488
20	0.9649	0.9643	1.0372	1.0190	0.9586	0.9587	1.0263	1.0093	1.2857	1.2844	0.8878	0.9874

Table 14
Effects of the use of varying number of vehicles on utilization rates and overall cost.

σ	F_D			F_L			F_E			F_C		
	n_v	r_u	Cost	n_v	r_u	Cost	n_v	r_u	Cost	n_v	r_u	Cost
6.40	3.00	21.99	1.0000	3.00	21.99	1.0159	3.00	21.99	1.0040	1.00	65.97	0.8692
58.53	3.00	26.70	1.0000	3.00	26.70	1.0048	3.00	26.70	0.9915	1.00	80.10	0.8444
122.22	3.00	31.88	1.0000	3.00	31.88	1.0066	3.00	31.88	0.9893	1.10	90.23	0.8830
180.22	3.00	36.59	1.0000	3.00	36.59	1.0171	3.00	36.59	0.9952	1.90	60.31	0.9198
227.23	3.00	40.41	1.0000	3.00	40.41	1.0100	3.00	40.41	1.0024	1.89	67.28	0.9395

This can be primarily explained by the increase in driver costs, where the average number of locations each driver visits increases with the number of locations in an instance. Conversely, for a fixed number of locations, the overall cost tends to increase with the number of vehicles. However, in this case driver costs tend to decrease (as each driver visits a fewer number of locations), but the substantial increase in CO_2 and fuel costs outweigh the decrease in driver costs and increase the overall cost. This is especially evident in the 15 and 20-node instances.

The final part of the analysis will look at the effect of using a variable number of vehicles in the routing, as mentioned in (ii) above. From a financial perspective, it is clear that the overall cost will increase with the number of vehicles used in the solution. Furthermore, as was illustrated in Section 3.5, varying the number of vehicles will have implications on vehicle utilization. It is difficult to incorporate the cost of vehicle acquisiton into formulations F_D, F_L and F_E due to the nature of their respective objective functions. However, this is straightforward with F_C, as discussed in Section 4, by treating the number of vehicles as a decision variable. If the vehicles are hired, rather than acquired, then the cost of the vehicles (e.g., hourly) can be incorporated into p. In this case, it suffices to replace constraints (10) with $\sum_{j \in \mathcal{N}} x_{0j} \leqslant m$, where m is an upper bound on the number of vehicles that can be used.

To provide further insights into these issues, we present in Table 14 the results of a set of experiments using a set of 15-node instances with time windows. For F_D, F_L and F_E, we use three vehicles of 3 t capacity each. For F_C, we allow the use of at most three vehicles with the hourly cost of a vehicle set at £55, an average quote in the UK obtained from the website of a commercial vehicle rental company. Customer demands are increased, as was done in Section 5.3, to analyze the utilization rates of the vehicles under changing demand values. The first column of Table 14 shows the standard deviation of the demands. The remaining rows show, for each model, the average number of vehicles used in the solution (n_v), the average utilization rates (r_u, in %) and the average standardized total costs (Cost). Each row of the table presents averages of the results on 10 instances.

The results in Table 14 show that formulations F_D, F_L and F_E have the same number of vehicles and utilization rates, and the overall costs produced by the three formulations are similar. Contrary to the other three formulations, the results indicate that F_C is not only able to reduce the overall cost but also able to increase the utilization ratios by using as few vehicles as possible in the routing.

6. Conclusions

We have introduced, modeled and analyzed the PRP, a variant of the well-known VRP, which considers, among other factors, an important side effect of vehicle transportation, namely CO_2 emissions. The contributions of this paper were: (i) to describe a modeling approach for incorporating fuel consumption and CO_2 emissions into existing planning methods for vehicle routing, (ii) to offer new integer programming formulations for the VRP which, in contrast to most of the existing studies, minimizes a total cost function composed of labor, fuel and emission costs expressed as a function of load, speed and other parameters, (iii) to present extensive computational analyses that capture the tradeoff between various performance measures. Results of the computational experiments on realistic instances yielded the following important conclusions:

- Minimizing emissions does not tell the whole story from a cost perspective; there are other factors to take into account such as labor costs which seem to dominate the overall cost. Based on the current estimates, the cost of CO_2 emissions does not seem to be as important as fuel or labor costs. However, our model provides a useful tool to evaluate the impact of energy reduction incentives, such as carbon taxes.
- The traditional objective of distance minimization does not necessarily imply minimization of either fuel cost or driver cost. In contrast, a cost-minimizing solution does not imply an energy-minimized solution. In fact, it implies a solution where more energy is consumed (hence yielding an increased amount of fuel consumption and emissions) in order to bring down driver costs. In a cost-minimized solution, the savings in driver costs can be up to 20%, resulting in a reduction of 5–8% in the overall cost (depending on the engine efficiency, and on the type of time window restrictions), compared to solutions obtained by other objectives.
- Minimizing the cumulative load only does not necessarily imply energy minimization, particularly when there are time window restrictions. An energy minimizing solution can make a significant difference in reducing energy requirements especially when time windows are in place (up to 10%) and when they are not tight enough to dictate a single solution.

- There is more room to reduce the energy consumption when the variation in demand is high (up to 4%), especially for the case where relatively few customers have significantly high amounts of demand compared to the rest. A similar argument can be made for the case where the load carried by the vehicle is close to its curb weight.
- The use of fewer vehicles generally implies a lower fuel consumption and a higher utilization rate of the vehicle capacity.
- Advances in engine technology make a difference in lowering the amount and cost of emissions and open opportunities to balance these costs against those of drivers, hence lowering the overall total cost. However, this only has a partial effect since driver costs are in any case the dominating component of the total cost which can be lowered by reducing the time spent on the route.

Several extensions are possible for the PRP. One worth mentioning here is the possibility of using a heterogeneous or mixed fleet of vehicles (Baldacci et al., 2008). Indeed, the flexibility afforded by the use of different vehicles may yield further reductions in energy consumption, total cost and vehicle utilization. Another extension would be to consider the time-dependent version of the problem, in particular where there are congested roads and one attempts to avoid congestion (Maden et al., 2010). We have mentioned above that our treatment of the problem assumed a free-flow speeds of at least 40 km/h. In congested environments where speed is often less than 40 km/h, acceleration and deceleration caused by frequent stops are the main contributors to emissions. Congestion is dynamic and stochastic and requires a treatment at a microscale level. Techniques like queueing analysis (see, e.g., Vandaele et al., 2000 and Van Woensel et al., 2001) would seem appropriate in this context.

Acknowledgements

References

Akçelik, R., Besley, M., 2003. Operating cost, fuel consumption, and emission models in aaSIDRA and aaMOTION. In: 25th Conference of Australian Institutes of Transport Research (CAITR 2003). University of South Australia, Adelaide, Australia.

Baldacci, R., Battarra, M., Vigo, D., 2008. Routing a heterogeneous fleet of vehicles. In: Golden, B.L., Raghavan, S., Wasil, E.A. (Eds.), The Vehicle Routing Problem: Latest Advances and New Challenges. Springer, New York, pp. 3–27 (Chapter 1).

Barth, M., Boriboonsomsin, K., 2008. Real-world CO_2 impacts of traffic congestion. Tech. rep., Paper for the 87th Annual Meeting of Transportation Research Board. <http://www.uctc.net/papers/846.pdf> (accessed 11.02.11).

Barth, M., Boriboonsomsin, K., 2009. Energy and emissions impacts of a freeway-based dynamic eco-driving system. Transportation Research Part D 14 (6), 400–410.

Barth, M., Younglove, T., Scora, G., 2005. Development of a heavy-duty diesel modal emissions and fuel consumption model. Tech. rep. UCB-ITS-PRR-2005-1, California PATH Program, Institute of Transportation Studies, University of California at Berkeley.

Bauer, J., Bektaş, T., Crainic, T.G., 2010. Minimizing greenhouse gas emissions in intermodal freight transport: an application to rail service design. Journal of the Operational Research Society 61 (3), 530–542.

Coe, E., 2005. Average carbon dioxide emissions resulting from gasoline and diesel fuel. Tech. rep., United States Environmental Protection Agency. <http://www.epa.gov/otaq/climate/420f05001.pdf> (accessed 11.02.11).

Cordeau, J.-F., Laporte, G., Savelsbergh, M.W.P., Vigo, D., 2007. Vehicle routing. In: Barnhart, C., Laporte, G. (Eds.), Transportation, Handbooks in Operations Research and Management Science, vol. 14. Elsevier, Amsterdam, The Netherlands, pp. 367–428 (Chapter 6).

Cornillier, F., Laporte, G., Boctor, F.F., Renaud, J., 2009. The petrol station replenishment problem with time windows. Computers & Operations Research 36 (3), 919–935.

DEFRA, 2007. The social cost of carbon and the shadow price of carbon: what they are, and how to use them in economic appraisal in the UK. Tech. rep., Department for Environment, Food, and Rural Affairs – Economics Group. <http://www.decc.gov. uk/en/content/cms/what_we_do/lc_uk/valuation/ shadow%_price/shadow_price.aspx> (accessed 11.02.11).

Desrochers, M., Laporte, G., 1991. Improvements and extensions to the Miller–Tucker–Zemlin subtour elimination constraints. Operations Research Letters 10 (1), 27–36.

Fagerholt, K., Laporte, G., Norstad, I., 2010. Reducing fuel emissions by optimizing speed on shipping routes. Journal of the Operational Research Society 61 (3), 523–529.

Forkenbrock, D.J., 2001. Comparison of external costs of rail and truck freight transportation. Transportation Research Part A 35 (4), 321–337.

Genta, G., 1997. Motor Vehicle Dynamics: Modelling and Simulation. World Scientific Publishing, Singapore.

Golden, B.L., Raghavan, S., Wasil, E.A., 2008. The Vehicle Routing Problem: Latest Advances and Recent Challenges. Operations Research Computer Science Interfaces. Springer, New York.

Hsu, C.-I., Hung, S.-F., Li, H.-C., 2007. Vehicle routing problem with time-windows for perishable food delivery. Journal of Food Engineering 80 (2), 465–475.

Jabali, O., Van Woensel, T., de Kok, A.G., 2009. Analysis of travel times and CO_2 emissions in time-dependent vehicle routing. Tech. rep., Eindhoven University of Technology.

Kara, I., Kara, B.Y., Yetis, M.K., 2007. Energy minimizing vehicle routing problem. In: Dress, A., Xu, Y., Zhu, B. (Eds.), Combinatorial Optimization and Applications, Lecture Notes in Computer Science, vol. 4616. Springer, Berlin/Heidelberg, pp. 62–71.

Knörr, W., 2008. EcoTransIT: ecological transport information tool – environmental methodology and data. Tech. rep., Institut für Energie (ifeu) und Umweltforschung Heidelberg GmbH, <http://www.ecotransit.org/download/ecotransit_background_report.pdf> (accessed 11.02.11).

Kreith, F., West, R.E., July 2003. Gauging Efficiency, Well to Wheel. Mechanical Engineering. <http://www.memagazine.org/supparch/mepower03/gauging/ gauging.html> (accessed 11.02.09).

Maden, W., Eglese, R.W., Black, D., 2010. Vehicle routing and scheduling with time varying data: a case study. Journal of the Operational Research Society 61 (3), 515–522.

McKinnon, A., 2007. CO_2 Emissions from freight transport in the UK. Tech. rep., Prepared for the Climate Change Working Group of the Commission for Integrated Transport, London, UK. <www.isotrak.com/news/press/CO2_emissions_freight_transport.pdf> (accessed 11.02.11).

Mima, S., Criqui, P., 2003. The future of fuel cells in a long term inter-technology competition network. In: Avadikyan, A., Cohendet, P., Heraud, J.-A. (Eds.), The Economic Dynamics of Fuel Cell Technologies. Springer, Berlin/Heidelberg, pp. 43–77 (Chapter 2).

Ohnishi, H., 2008. Greenhouse Gas Reduction Strategies in the Transport Sector: Preliminary Report. Tech. rep., OECD/ITF Joint Transport Research Centre Working Group on GHG Reduction Strategies in the Transport Sector, OECD/ITF, Paris. <http://www.internationaltransportforum.org/Pub/pdf/08GHG.pdf> (accessed 11.02.11).

Palmer, A., 2007. The Development of an integrated routing and carbon dioxide emissions model for goods vehicles. Ph.D. thesis, Cranfield University, School of Management.

Payscale, 2009a. <http://www.payscale.com/research/UK/Job=Truck_Driver,_Heavy_%2 F_Tractor%-Trailer/Hourly_Rate> (as of 5.10.09).

Payscale, 2009b. <http://www.payscale.com/research/US/Job=Truck_Driver,_Heavy_%2 F_Tractor%-Trailer/Hourly_Rate> (as of 5.10.09).

Ross, M., 1997. Fuel efficiency and the physics of automobiles. Contemporary Physics 38 (6), 381–394.

Sbihi, A., Eglese, R.W., 2007. Combinatorial optimization and green logistics. 4OR: A Quarterly Journal of Operations Research 5 (2), 99–116.

Simpson, A.G., February 2005. Parametric modelling of energy consumption in road vehicles. Ph.D. thesis, The University of Queensland, School of Information Technology and Electrical Engineering. <http://www.itee.uq.edu.au/serl/_pamvec/PhD_Thesis_AGS_050420.pdf> (accessed 11.02.11).

The Automobile Association Limited, 2009. Fuel price reports. <http://www.theaa.com/motoring_advice/fuel/> (as of 5.10.09).

Tol, R.S.J., 2005. The marginal damage costs of carbon dioxide emissions: an assessment of the uncertainties. Energy Policy 33 (16), 2064–2074.

Van Woensel, T., Creten, R., Vandaele, N., 2001. Managing the environmental externalities of traffic logistics: the issue of emissions. Production and Operations Management 10 (2), 207–223.

Vandaele, N., Van Woensel, T., Verbruggen, A., 2000. A queueing based traffic flow model. Transportation Research Part D 5 (2), 121–135.

Wikipedia, 2009. Truck classification. <http://en.wikipedia.org/wiki/Truck_classification> (accessed 11.02.11).